

Ruthenium(II) complexes containing novel asymmetric tridentate ligands: synthesis, structure, electrochemical and spectroscopic properties

Hui Chao,^a Guang Yang,^a Gen-Qiang Xue,^a Hong Li,^a Hao Zang,^a Ian D. Williams,^b Liang-Nian Ji,^{*a} Xiao-Ming Chen^a and Xiao-Yuan Li^{*b}

^a State Key Laboratory of Ultrafast Laser Spectroscopy/Department of Chemistry, Zhongshan University, Guangzhou 510275, P. R. China. E-mail: cesjln@zsu.edu.cn

^b Department of Chemistry, Hong Kong University of Science and Technology, Kowloon, Hong Kong, P. R. China. E-mail: chxyli@ust.hk

Received 4th December 2000, Accepted 21st February 2001

First published as an Advance Article on the web 27th March 2001

Three novel asymmetrical tridentate ligands, 3-(1,10-phenanthroline-2-yl)-5,6-diphenyl-*as*-triazine (dppt), 3-(1,10-phenanthroline-2-yl)-*as*-triazino[5,6-*f*]acenaphthylene (pta) and 3-(1,10-phenanthroline-2-yl)-*as*-triazino[5,6-*f*]phenanthrene (ptp) have been prepared. Their homoleptic ruthenium complexes [Ru(L)₃]²⁺ (L = dppt, pta or ptp) and heteroleptic ruthenium complexes [Ru(tpy)(L)]²⁺ have been synthesized and characterized by ¹H NMR, ES-MS, electronic absorption spectroscopy and cyclic voltammetry. The heteroleptic ruthenium complexes were also characterized by X-ray crystallography. The electrochemical and spectroscopic studies of the complexes display the changes in properties in comparison with [Ru(tpy)₃]²⁺ owing to the structural differences.

The modification or fine tuning of the electronic and redox properties of ruthenium(II) complexes has received much attention with regard to photochemical molecular devices for energy conversion and photoinduced electron transfer.¹ However, most studies have primarily focused on complexes involving bidentate ligands such as 2,2'-bipyridine (bpy) and 1,10-phenanthroline (phen). Over the past decade quite a large amount of data has been accumulated on the changes in the electrochemical and photophysical properties of complexes effected by substitution in the bpy or phen rings, or replacement of one or both of the pyridine rings with other nitrogen-containing heterocycles.¹ On the other hand, there are relatively fewer ruthenium complexes with tridentate ligands because interest in such complexes is restricted by the absence of room temperature luminescence of [Ru(tpy)₃]²⁺ (tpy = 2,2':6',2''-terpyridine).² Few ligands other than tpy have been used in this regard until recently.²⁻¹² Most of those reported tridentate ligands are symmetrical or essentially symmetrical aromatic ligands and use of them presents an opportunity to avoid the stereochemical problem existing in octahedral complexes with bidentate ligands. On the contrary, by having asymmetric tridentate ligands, chirality is reintroduced to the octahedral complexes. Until now, ruthenium(II) complexes with asymmetric tridentate ligands are scarcely known.¹³

In order to obtain more insight into the properties of ruthenium complexes with asymmetric tridentate ligands, we have recently designed three novel asymmetric tridentate ligands, 3-(1,10-phenanthroline-2-yl)-5,6-diphenyl-*as*-triazine (dppt), 3-(1,10-phenanthroline-2-yl)-*as*-triazino[5,6-*f*]acenaphthylene (pta) and 3-(1,10-phenanthroline-2-yl)-*as*-triazino[5,6-*f*]phenanthrene (ptp). Both the asymmetry and the extended π framework of the new ligands will have a different effect on the properties of ruthenium complexes in comparison with tpy and its derivatives. In the present study the homoleptic ruthenium complexes [Ru(L)₃]²⁺ (L = dppt, pta or ptp) and heteroleptic ruthenium complexes [Ru(tpy)(L)]²⁺ have been synthesized and characterized by spectral and electrochemical methods. To ascertain the nature of the coordination mode of the asymmetric ligands the crystal structures of the heteroleptic ruthenium complexes have been determined.

Experimental

Syntheses

The compounds [Ru(tpy)Cl₃]¹⁴ and 2-cyano-1,10-phenanthroline¹⁵ were prepared according to the literature procedures. Other materials were commercially available and of reagent grade.

2-Amino(hydrazono)methyl-1,10-phenanthroline (PNH). A mixture of 2-cyano-1,10-phenanthroline (2.4 mmol, 0.5 g), ethanol (10 cm³) and 40% hydrazine (4 cm³) was stirred at room temperature for 3 h. Evaporation of the solution gave 0.563 g (86%) of PNH as yellow needles (Found: C, 56.81; H, 5.41; N, 25.33. Calc. for C₁₃H₁₁N₅·2H₂O: C, 56.93; H, 5.84; N, 25.55%). ¹H NMR [(CD₃)₂SO]: δ 9.14 (d, 1H, *J* = 5), 8.48 (d, 1H, *J* = 8), 8.38 (d, 1H, *J* = 8), 8.29 (d, 1H, *J* = 8.5), 7.97 (d, 1H, *J* = 9), 7.95 (d, 1H, *J* = 8.5 Hz), 7.77 (dd, 1H), 6.06 (s, 2H) and 5.61 (s, 2H). FAB-MS: *m/z* = 238 (C₁₃H₁₁N₅ requires 237).

dppt. A mixture of PNH (0.263 g, 0.96 mmol) and benzil (0.2 g, 0.95 mmol) was refluxed with stirring in ethanol for 3 h. After cooling to room temperature, the solution was then poured into water and the precipitate removed by filtration and dried at 50 °C *in vacuo*. Yield: 0.312 g, 80% (Found: C, 73.85; H, 4.62; N, 15.80. Calc. for C₂₇H₁₇N₅·1.5H₂O: C, 73.97; H, 4.57; N, 15.98%). ¹H NMR [(CD₃)₂SO]: δ 9.17 (d, 1H, *J* = 6), 8.86 (d, 1H, *J* = 8.5), 8.76 (d, 1H, *J* = 8.5), 8.54 (d, 1H, *J* = 8), 8.12 (s, 2H), 7.82 (dd, 1H), 7.67 (d, 2H, *J* = 7.5), 7.63 (d, 2H, *J* = 7.5 Hz), 7.52 (t, 1H), 7.50 (t, 2H), 7.49 (t, 1H) and 7.45 (t, 2H). FAB-MS: *m/z* = 412 (C₂₇H₁₇N₅ requires 411).

pta. A mixture of PNH (0.263 g, 0.96 mmol) and acenaphthenequinone (0.173 g, 0.95 mmol) was refluxed in ethanol. In a few minutes much yellow precipitate appeared. After 3 h stirring the insoluble material was removed by filtration while hot, washed with ethanol (3 \times 5 cm³), then dried at 50 °C *in vacuo*. Yield: 0.244 g, 67% (Found: C, 71.20; H, 4.44; N, 16.38. Calc. for C₂₅H₁₃N₅·2H₂O: C, 71.60; H, 4.06; N, 16.71%). ¹H NMR [(CD₃)₂SO]: δ 9.21 (d, 1H, *J* = 6), 8.89 (d, 1H, *J* = 8), 8.75 (d, 2H, *J* = 7.5), 8.66 (d, 1H, *J* = 7), 8.54 (d, 1H, *J* = 8), 8.52 (d, 1H,

$J = 8$), 8.44 (d, 1H, $J = 8.5$ Hz), 8.11 (s, 2H), 8.08 (t, 1H), 8.05 (t, 1H) and 7.84 (dd, 1H). FAB-MS: $m/z = 384$ ($C_{25}H_{13}N_5$ requires 383).

ptp. This compound was synthesized in an identical manner to that described for pta, with 0.95 mmol, 0.198 g phenanthrene-5,6-dione in place of acenaphthenequinone. Yield 0.291 g, 75% (Found: C, 75.60; H, 4.14; N, 16.38. Calc. for $C_{27}H_{15}N_5 \cdot H_2O$: C, 75.88; H, 3.98; N, 16.39%). 1H NMR $[(CD_3)_2SO]$: δ 9.45 (d, 1H, $J = 6$), 9.44 (d, 1H, $J = 6.5$), 9.23 (d, 1H, $J = 6$), 9.05 (d, 1H, $J = 8.5$), 8.90 (d, 2H, $J = 8$), 8.80 (d, 1H, $J = 8.5$), 8.55 (d, 1H, $J = 8.5$ Hz), 8.12 (s, 2H), 8.05 (t, 1H), 8.00 (t, 1H), 7.94 (t, 2H) and 7.85 (dd, 1H). FAB-MS: $m/z = 410$ ($C_{27}H_{15}N_5$ requires 409).

[Ru(dppt)] $_2$ [ClO $_4$] $_2$ 1. A mixture of dppt (0.15 g, 0.367 mmol) and $RuCl_3 \cdot 3H_2O$ (0.048 g, 0.183 mmol) in absolute ethanol (30 cm 3) was refluxed for 10 h. After being cooled to room temperature, the reaction mixture was filtered. Excess of $NaClO_4$ in ethanol was added to the filtrate. The brownish red precipitate formed was collected and purified by column chromatography on alumina with acetonitrile–toluene (2 : 1 v/v) as eluent. Yield: 0.146 g, 70% (Found: C, 56.4; H, 3.1; N, 12.0. Calc. for $C_{54}H_{34}Cl_2N_{10}O_8Ru \cdot H_2O$: C, 56.8; H, 3.0; N, 12.3%). MS [ESMS (CH_3OH)]: m/z 1025.1 ($[M - ClO_4]^+$) and 462.3 ($[M - 2ClO_4]^{2+}$). 1H NMR $[(CD_3)_2SO]$: δ 9.25 (d, 2H, $J = 7$), 9.18 (d, 2H, $J = 7$), 8.72 (d, 2H, $J = 7$), 8.66 (d, 2H, $J = 8$), 8.48 (d, 2H, $J = 7.5$), 8.32 (d, 2H, $J = 5$), 7.62 (dd, 2H), 7.56 (d, 2H, $J = 6$ Hz), 7.51 (t, 4H), 7.40 (t, 4H), 7.32 (t, 4H), 7.16 (t, 4H) and 6.80 (d, 2H).

[Ru(pta) $_2$][ClO $_4$] $_2$ 2. This complex was synthesized in an identical manner to that described for $[Ru(dppt)_2][ClO_4]_2$, with 0.367 mmol, 0.141 g pta in place of dppt. Yield 0.094 g, 48% (Found: C, 54.3; H, 2.6; N, 12.5. Calc. for $C_{50}H_{28}Cl_2N_{10}O_8Ru \cdot 2H_2O$: C, 54.4; H, 2.7; N, 12.7%). MS [ESMS (CH_3OH)]: m/z 967.1 ($[M - ClO_4]^+$) and 434.2 ($[M - 2ClO_4]^{2+}$). 1H NMR $[(CD_3)_2SO]$: δ 9.37 (d, 2H, $J = 7$), 9.30 (d, 2H, $J = 7$), 8.75 (d, 2H, $J = 7.5$), 8.72 (d, 2H, $J = 6.5$), 8.67 (d, 2H, $J = 6$), 8.52 (d, 2H, $J = 7.5$), 8.44 (d, 2H, $J = 6.5$), 8.34 (d, 2H, $J = 6.5$), 8.26 (d, 2H, $J = 4$ Hz), 8.03 (t, 2H), 7.86 (t, 2H), 7.80 (t, 2H) and 7.61 (dd, 2H).

[Ru(ptp) $_2$][ClO $_4$] $_2$ 3. This complex was synthesized in an identical manner to that described for $[Ru(dppt)_2][ClO_4]_2$, with 0.367 mmol, 0.15 g ptp in place of dppt. Yield 0.108 g, 52% (Found: C, 56.7; H, 3.0; N, 12.1. Calc. for $C_{54}H_{30}Cl_2N_{10}O_8Ru \cdot H_2O$: C, 57.0; H, 2.8; N, 12.3%). MS [ESMS (CH_3OH)]: m/z 1018.9 ($[M - ClO_4]^+$) and 460.4 ($[M - 2ClO_4]^{2+}$). 1H NMR $[(CD_3)_2SO]$: δ 9.60 (d, 2H, $J = 8$), 9.41 (d, 2H, $J = 5.5$), 9.40 (d, 2H, $J = 3.5$), 8.80 (d, 2H, $J = 3.5$), 8.76 (d, 2H, $J = 8.5$), 8.74 (d, 2H, $J = 8$), 8.69 (d, 2H, $J = 8$), 8.57 (d, 2H, $J = 8.5$), 8.47 (d, 2H, $J = 5$), 7.98 (t, 2H), 7.90 (t, 2H), 7.82 (t, 2H), 7.66 (d, 2H, $J = 6.5$ Hz), 7.65 (t, 2H) and 7.56 (t, 2H).

[Ru(tpy)(dppt)][ClO $_4$] $_2$ 4. A mixture of $Ru(tpy)Cl_3$ (0.1 g, 0.227 mmol), dppt (0.093 g, 0.227 mmol) and triethylamine (1 cm 3) in ethanol–water (1 : 1 v/v, 50 cm 3) was refluxed for 10 h, during which time the solution turned dark purple. After being cooled to room temperature, a dark red precipitate was obtained by addition of aqueous $NaClO_4$ solution. The product was purified by column chromatography on alumina with acetonitrile–toluene (1 : 1 v/v) as eluent. Yield: 0.096 g, 45%. Single crystals suitable for an X-ray crystallographic study were grown from acetonitrile–toluene (1 : 1, v/v) at room temperature. Found: C, 53.6; H, 2.7; N, 12.3. Calc. for $C_{42}H_{28}Cl_2N_8O_8Ru$: C, 53.4; H, 3.0; N, 11.9%). MS [ESMS (CH_3OH)]: m/z 844 ($[M - ClO_4]^+$) and 373 ($[M - 2ClO_4]^{2+}$). 1H NMR $[(CD_3)_2SO]$: δ 9.22 (d, 1H, $J = 8.5$), 9.13 (d, 1H, $J = 9$), 9.05 (d, 1H, $J = 8$), 8.78 (d, 2H, $J = 8$), 8.74 (d, 1H, $J = 8.5$), 8.67 (d, 1H,

$J = 9$), 8.57 (t, 1H), 8.50 (d, 1H, $J = 9$), 8.25 (d, 1H, $J = 5.5$), 8.00 (t, 2H), 7.67 (dd, 1H), 7.59 (d, 2H, $J = 7.5$), 7.51 (t, 1H), 7.40 (m, 3H), 7.35 (d, 2H, $J = 5$), 7.27 (t, 2H), 7.16 (t, 2H) and 7.05 (d, 2H, $J = 8$ Hz).

[Ru(tpy)(pta)][ClO $_4$] $_2$ 5. This complex (dark brown) was synthesized in an identical manner to that described for $[Ru(tpy)(dppt)][ClO_4]_2$, with 0.227 mmol, 0.087 g pta in place of dppt. Yield 0.106 g, 51%. Single crystals suitable for an X-ray crystallographic study were grown from acetonitrile–toluene (1 : 1, v/v) at room temperature. Found: C, 53.0; H, 2.6; N, 13.4. Calc. for $C_{40}H_{24}Cl_2N_8O_8Ru \cdot CH_3CN$: C, 52.7; H, 2.8; N, 13.2%). MS [ESMS (CH_3OH)]: m/z 817 ($[M - ClO_4]^+$) and 358 ($[M - 2ClO_4]^{2+}$). 1H NMR $[(CD_3)_2SO]$: δ 9.28 (d, 1H, $J = 8.5$), 9.15 (dd, 3H), 8.83 (d, 2H, $J = 8$), 8.70 (m, 4H), 8.49 (d, 2H, $J = 8$), 8.41 (d, 1H, $J = 8$), 8.19 (d, 1H, $J = 5$), 8.07 (t, 2H), 7.98 (t, 2H), 7.89 (t, 1H), 7.67 (dd, 1H), 7.34 (d, 2H, $J = 5$ Hz) and 7.13 (t, 2H).

[Ru(tpy)(ptp)][ClO $_4$] $_2$ 6. This complex (dark brown) was synthesized in an identical manner to that described for $[Ru(tpy)(dppt)][ClO_4]_2$, with 0.227 mmol, 0.087 g ptp in place of dppt. Yield 0.099 g, 39%. Single crystals suitable for an X-ray crystallographic study were grown from acetonitrile–toluene (1 : 1, v/v) at room temperature. Found: C, 52.6; H, 2.7; N, 11.8. Calc. for $C_{42}H_{26}Cl_2N_8O_8Ru \cdot H_2O$: C, 52.5; H, 2.9; N, 11.7%). MS [ESMS (CH_3OH)]: m/z 843 ($[M - ClO_4]^+$) and 372 ($[M - 2ClO_4]^{2+}$). 1H NMR $[(CD_3)_2SO]$: δ 9.50 (d, 1H, $J = 9$), 9.42 (d, 1H, $J = 8$), 9.22 (d, 1H, $J = 8$), 9.17 (d, 2H, $J = 8$), 8.83 (d, 2H, $J = 8$), 8.74 (m, 5H), 8.54 (d, 1H, $J = 9$), 8.38 (d, 1H, $J = 5$), 8.18 (d, 1H, $J = 8$), 7.99 (m, 3H), 7.93 (t, 1H), 7.90 (t, 1H), 7.72 (t, 1H), 7.70 (d, 1H, $J = 6$), 7.39 (d, 2H, $J = 6$ Hz) and 7.13 (t, 2H).

CAUTION: perchlorate salts of metal complexes with organic ligands are potentially explosive, and only small amounts of the material should be prepared and handled with great care.

Physical measurements

The analyses (C, H and N) were performed using a Perkin-Elmer 240Q elemental analyser. Absorption spectra were recorded on a Shimadzu MPS-2000 spectrophotometer, 1H NMR spectra on Varian INOVA-500 and Bruker AMX-600 spectrometers with $(CD_3)_2SO$ as solvent at room temperature and $SiMe_4$ as an internal standard and fast atom bombardment (FAB) mass spectra on a VG ZAB-HS spectrometer in a 3-nitrobenzyl alcohol matrix. Electrospray (ES) mass spectra were recorded on a LCQ system (Finnigan MAT, USA) using methanol as mobile phase. The spray voltage, tube lens offset, capillary voltage and capillary temperature were set at 4.50 kV, 30.00 V, 23.00 V and 200 °C, respectively, and the quoted m/z values are for the major peaks in the isotope distribution.

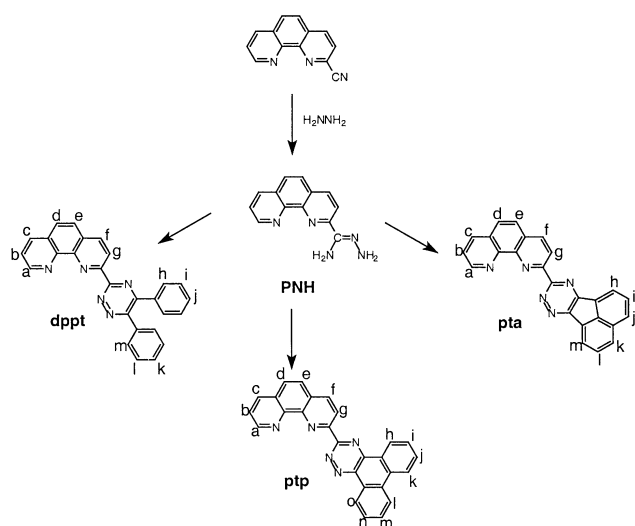
Cyclic voltammetry was performed on an EG&G PAR 273 polarographic analyser and 270 universal programmer. The supporting electrolyte was 0.1 mol dm $^{-3}$ tetrabutylammonium perchlorate in acetonitrile freshly distilled from phosphorus pentaoxide and deaerated by purging with nitrogen. A standard three-electrode system was used comprising a platinum microcylinder working electrode, platinum-wire auxiliary electrode and a saturated calomel reference electrode (SCE).

X-Ray crystallography

A summary of pertinent crystallographic data and experimental details for **4**, **5** and **6** is shown in Table 1. Diffraction intensities for complexes **4** and **6** were collected on a Siemens R3m diffractometer using the ω -scan technique. Lorentz-polarization and absorption corrections were applied.¹⁶ Diffraction intensities for **5** were collected (hemisphere technique) on a Bruker SMART Platform CCD diffractometer and an absorp-

Table 1 Crystal data and structural refinement for complexes **4**, **5** and **6**

	4	5	6
Chemical formula	C ₄₂ H ₂₈ Cl ₂ N ₈ O ₈ Ru	C ₄₂ H ₂₇ Cl ₂ N ₉ O ₈ Ru	C ₄₂ H ₂₈ Cl ₂ N ₈ O ₉ Ru
Formula weight	944.69	957.71	960.71
Crystal system	Triclinic	Monoclinic	Monoclinic
Space group	<i>P</i> $\bar{1}$	<i>P</i> 2 ₁ / <i>n</i>	<i>P</i> 2 ₁ / <i>n</i>
<i>a</i> /Å	11.0480(10)	12.3635(19)	14.758(7)
<i>b</i> /Å	12.9520(10)	26.210(4)	16.920(7)
<i>c</i> /Å	15.721(2)	12.4622(19)	16.887(4)
β /°	73.610(10)	102.797(3)	90.68
<i>V</i> /Å ³	1964.3(3)	3938.0(11)	4216(3)
<i>Z</i>	2	4	4
μ /mm ⁻¹	0.602	0.605	0.564
<i>T</i> /K	293(2)	293(2)	293(2)
Measured/independent reflections and <i>R</i> (int)	6785, 6396, 0.0709	28124, 11384, 0.0288	7712, 7417, 0.0384
<i>R</i> 1 [<i>I</i> > 2 σ (<i>I</i>)]	0.0575	0.0487	0.0793
<i>wR</i> 2 (all data)	0.1430	0.1598	0.2407

**Scheme 1** Synthetic routes for the preparation of the ligands.

tion correction was applied with the SADABS program.¹⁷ The structure solution and full-matrix least-squares refinement based on *F*² for **4**, **5** and **6** were performed with the SHELXS 97 and SHELXL 97¹⁸ program packages, respectively. All the non-hydrogen atoms were refined anisotropically. Hydrogen atoms of the organic ligands were generated geometrically (C–H 0.96 Å).

CCDC reference numbers 154059–154061.

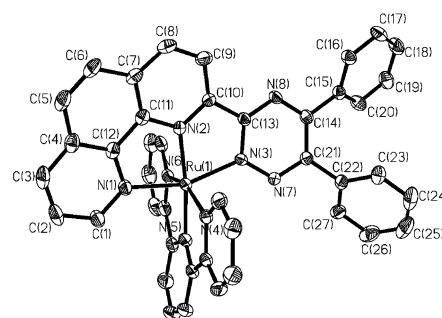
See <http://www.rsc.org/suppdata/dt/b0/b009680f/> for crystallographic data in CIF or other electronic format.

Results and discussion

Syntheses

The outline of the syntheses of the ligands is presented in Scheme 1. The ligands were synthesized on the basis of the method for the 1,2,4-triazine ring preparation established by Case.¹⁹ By the action of an ethanol solution of hydrazine, 2-cyano-1,10-phenanthroline was converted into PNH (86% yield). Refluxing of the latter with an ethanol solution of benzil produced dppt in 80% yield. Similar treatment with acenaphthenequinone afforded pta (67% yield). Reaction of phenanthrene-5,6-dione with PNH yielded ptp (75% yield).

Homoleptic ruthenium complexes [RuL₂][ClO₄]₂ (L = dppt, pta or ptp) were obtained from RuCl₃·3H₂O with 2 equivalents of the ligand in boiling ethanol, followed by chromatography [alumina, acetonitrile–toluene (2 : 1 v/v) as eluent] and metathesis with NaClO₄. Yields were in the range 48–70%. Reactions of 1 equivalent of the appropriate ligand with Ru-

**Fig. 1** An ORTEP drawing of [Ru(tpy)(dppt)]²⁺ and the atom numbering.

(tpy)Cl₃ in aqueous ethanol at reflux in the presence of an excess of triethylamine for 10 h, followed by metathesis with NaClO₄, afforded the heteroleptic ruthenium complexes [Ru(tpy)L][ClO₄]₂ (L = dppt, pta or ptp). These were also purified by column chromatography [alumina, acetonitrile–toluene (1 : 1 v/v) as eluent].

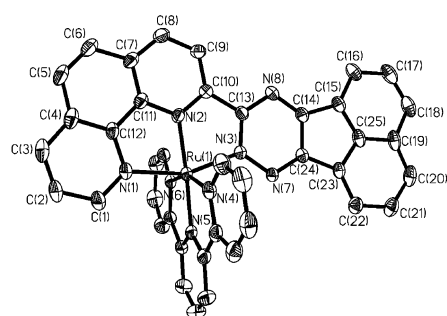
Structural analyses

[Ru(tpy)(dppt)][ClO₄]₂ 4. The crystal structure of complex **4** consists of a [Ru(tpy)(dppt)]²⁺ cation and two disordered ClO₄[−] anions in an asymmetric unit. An ORTEP²⁰ view of the cation is illustrated in Fig. 1. Selected bond lengths and angles are presented in Table 2.

As shown in Fig. 1, the ruthenium(II) ion displays the expected distorted-octahedral geometry with intraligand bite angles in the range 77.08–79.95°, and the two tridentate ligands coordinate in the meridional fashion. All C–N and C–C distances are in the normal range. The ligand dppt can coordinate to metal ions *via* two different sites, N(3) of the 1,2,4-triazine ring and the nitrogen atoms of the phen ring or N(8) of the 1,2,4-triazine ring and the nitrogen atoms of the phen ring. The structure confirms that the coordination is at N(3) rather than N(8) due to the steric hindrance between the ligands. Owing to the constrained bite of the ligands, the Ru–N bond lengths to the central ring [1.973(4)–1.989(4) Å] are shorter than those to the terminal rings [2.067(5)–2.105(4) Å], which is typical for coordination of conjugated terimine systems.^{4,12,21} It is interesting that the two ligands, dppt and tpy, show different binding to the ruthenium ion. The two Ru–N (terminal pyridyl ring) distances of tpy are similar at 2.067(5) [Ru(1)–N(4)] and 2.073(5) [Ru(1)–N(6)]. However in dppt the two Ru–N (terminal ring) distances are significantly different. The N(1) atom in the phen ring is bound in a manner similar to that of a 1,10-phenanthroline ligand²² with Ru(1)–N(1) separation of 2.105(4) Å; the separation between Ru(1) and N(3) in the 1,2,4-triazine ring is contracted at 2.072(4) Å. This can be attributed

Table 2 Selected bond lengths (Å) and angles (°) for complex **4**, **5** and **6**

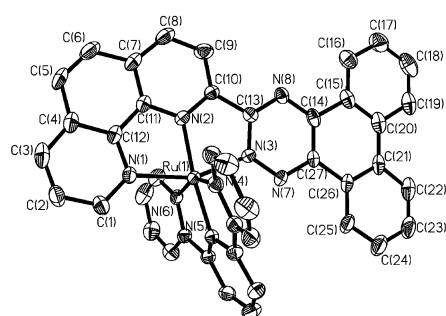
4					
Ru(1)–N(1)	2.105(4)	Ru(1)–N(2)	1.973(4)	Ru(1)–N(3)	2.072(4)
Ru(1)–N(4)	2.067(5)	Ru(1)–N(5)	1.989(4)	Ru(1)–N(6)	2.073(5)
N(2)–Ru(1)–N(5)	173.64(18)	N(3)–Ru(1)–N(6)	93.38(17)	C(11)–N(2)–Ru(1)	117.0(4)
N(2)–Ru(1)–N(4)	99.57(18)	N(2)–Ru(1)–N(1)	79.95(18)	N(7)–N(3)–Ru(1)	127.7(3)
N(5)–Ru(1)–N(4)	79.4(2)	N(5)–Ru(1)–N(1)	93.82(18)	C(13)–N(3)–Ru(1)	114.9(3)
N(2)–Ru(1)–N(3)	77.08(17)	N(4)–Ru(1)–N(1)	93.62(18)	C(28)–N(4)–Ru(1)	128.0(4)
N(5)–Ru(1)–N(3)	109.21(17)	N(3)–Ru(1)–N(1)	156.83(17)	C(32)–N(4)–Ru(1)	114.5(3)
N(4)–Ru(1)–N(3)	93.10(17)	N(6)–Ru(1)–N(1)	88.51(17)	C(37)–N(5)–Ru(1)	118.5(4)
N(2)–Ru(1)–N(6)	102.10(18)	C(1)–N(1)–Ru(1)	132.1(4)	C(33)–N(5)–Ru(1)	117.9(4)
N(5)–Ru(1)–N(6)	78.8(2)	C(12)–N(1)–Ru(1)	110.8(3)	C(42)–N(6)–Ru(1)	128.0(4)
N(4)–Ru(1)–N(6)	158.26(18)	C(10)–N(2)–Ru(1)	122.2(4)	C(38)–N(6)–Ru(1)	114.1(4)
5					
Ru(1)–N(1)	2.112(3)	Ru(1)–N(2)	1.971(3)	Ru(1)–N(3)	2.064(2)
Ru(1)–N(4)	2.072(3)	Ru(1)–N(5)	1.988(3)	Ru(1)–N(6)	2.074(3)
N(2)–Ru(1)–N(5)	175.44(11)	N(6)–Ru(1)–N(4)	157.33(12)	C(11)–N(2)–Ru(1)	118.3(2)
N(2)–Ru(1)–N(3)	77.42(10)	N(2)–Ru(1)–N(1)	79.26(11)	C(13)–N(3)–Ru(1)	114.92(19)
N(5)–Ru(1)–N(3)	104.75(10)	N(5)–Ru(1)–N(1)	98.67(10)	N(7)–N(3)–Ru(1)	124.92(19)
N(2)–Ru(1)–N(6)	97.31(11)	N(3)–Ru(1)–N(1)	156.58(11)	C(26)–N(4)–Ru(1)	127.9(3)
N(5)–Ru(1)–N(6)	78.73(11)	N(6)–Ru(1)–N(1)	94.23(10)	C(30)–N(4)–Ru(1)	114.5(2)
N(3)–Ru(1)–N(6)	90.83(10)	N(4)–Ru(1)–N(1)	91.85(10)	C(35)–N(5)–Ru(1)	119.3(2)
N(2)–Ru(1)–N(4)	105.28(12)	C(1)–N(1)–Ru(1)	131.9(3)	C(31)–N(5)–Ru(1)	119.0(2)
N(5)–Ru(1)–N(4)	78.77(12)	C(12)–N(1)–Ru(1)	110.8(2)	C(40)–N(6)–Ru(1)	127.4(2)
N(3)–Ru(1)–N(4)	92.20(10)	C(10)–N(2)–Ru(1)	121.1(2)	C(36)–N(6)–Ru(1)	114.0(2)
6					
Ru(1)–N(1)	2.130(7)	Ru(1)–N(2)	1.994(6)	Ru(1)–N(3)	2.042(6)
Ru(1)–N(4)	2.088(7)	Ru(1)–N(5)	2.000(6)	Ru(1)–N(6)	2.084(7)
N(2)–Ru(1)–N(5)	173.2(3)	N(6)–Ru(1)–N(4)	156.2(3)	C(10)–N(2)–Ru(1)	120.8(5)
N(2)–Ru(1)–N(3)	78.0(3)	N(2)–Ru(1)–N(1)	78.5(3)	N(7)–N(3)–Ru(1)	124.7(5)
N(5)–Ru(1)–N(3)	95.2(2)	N(5)–Ru(1)–N(1)	108.3(3)	C(13)–N(3)–Ru(1)	115.9(5)
N(2)–Ru(1)–N(6)	101.1(3)	N(3)–Ru(1)–N(1)	156.5(3)	C(28)–N(4)–Ru(1)	128.3(6)
N(5)–Ru(1)–N(6)	78.5(3)	N(6)–Ru(1)–N(1)	90.3(2)	C(32)–N(4)–Ru(1)	113.8(5)
N(3)–Ru(1)–N(6)	95.4(3)	N(4)–Ru(1)–N(1)	92.1(3)	C(33)–N(5)–Ru(1)	118.5(6)
N(2)–Ru(1)–N(4)	102.6(3)	C(1)–N(1)–Ru(1)	132.1(6)	C(37)–N(5)–Ru(1)	118.7(5)
N(5)–Ru(1)–N(4)	78.3(3)	C(12)–N(1)–Ru(1)	110.5(5)	C(42)–N(6)–Ru(1)	127.7(6)
N(3)–Ru(1)–N(4)	91.8(3)	C(11)–N(2)–Ru(1)	118.6(6)	C(38)–N(6)–Ru(1)	113.8(5)

**Fig. 2** An ORTEP drawing of $[\text{Ru}(\text{tpy})(\text{pta})]^{2+}$ and the atom numbering.

to the large asymmetry of the ligand dppt. The inequivalence of the two terminal Ru–N bonds in dppt also indicates that the 1,2,4-triazine group has a stronger coordination ability in comparison with that of the terminal pyridyl group. In addition, the two phenyl rings in dppt are rotated away from the 1,2,4-triazine ring with large dihedral angles (37.2 and 48.3°, respectively).

$[\text{Ru}(\text{tpy})(\text{pta})][\text{ClO}_4]_2 \cdot \text{CH}_3\text{CN}$ 5. The asymmetric unit of complex **5** contains a $[\text{Ru}(\text{tpy})(\text{pta})]^{2+}$ cation, two disordered ClO_4^- anions and an acetonitrile solvate molecule. An ORTEP²⁰ view of the cation is presented in Fig. 2; selected bond lengths and angles are in Table 2.

Like complex **4**, the ruthenium atom resides in a pseudo-octahedral environment with the two tridentate ligands chelating in meridional fashions. As expected, the Ru–N separations

**Fig. 3** An ORTEP drawing of $[\text{Ru}(\text{tpy})(\text{ptp})]^{2+}$ and the atom numbering.

are very similar to those of **4**. The most striking difference is seen in the inequivalence of the two terminal Ru–N bonds of the asymmetric ligand. In pta the two rotated phenyl rings are replaced with a naphthyl ring. It is nearly coplanar with the 1,2,4-triazine ring and they can construct a larger π framework compared to that of dppt. This results in elongation of the separation between Ru(1) and N(1) in the phen ring [2.112(3) Å] and contraction of the separation between Ru(1) and the N(3) in the 1,2,4-triazine ring [2.064(2) Å].

$[\text{Ru}(\text{tpy})(\text{ptp})][\text{ClO}_4]_2 \cdot \text{H}_2\text{O}$ 6. The structure of complex **6** contains a lattice water along with the cation and two disordered anions. Fig. 3 shows an ORTEP²⁰ view of the cation, while selected bond lengths and angles are presented in Table 2.

The structure is very similar to that of complex **5** except that the naphthyl ring is replaced with a biphenyl ring. As seen in

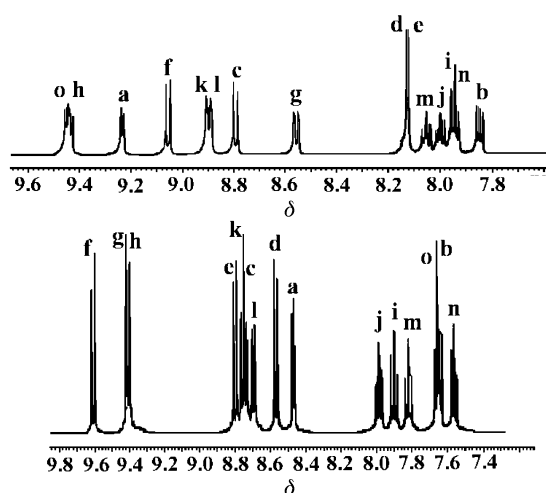


Fig. 4 The ^1H NMR spectra of ptp (top) and $[\text{Ru}(\text{ptp})_2]^{2+}$ (bottom) in the aromatic region between δ 7.0 and 10 $[(\text{CD}_3)_2\text{SO}$ solvent; TMS reference].

Table 2, the Ru(1)–N separations are very similar, the two terminal Ru–N bonds of the asymmetric ligand are still inequivalent, which is shown by the elongation of the separation between Ru(1) and the N(1) in the phen ring [2.130(7) Å] and the contraction of the separation between Ru(1) and the N(3) in the 1,2,4-triazine ring [2.042(6) Å]. This can be also attributed to the extension of the π delocalization. Judging from bond lengths, the inequivalence of the two terminal Ru–N bonds of the asymmetric ligand increases in the order: dppt < pta < ptp.

^1H NMR spectra

The asymmetric ligands and the ruthenium(II) complexes give well defined ^1H NMR spectra, which permit unambiguous identification and assessment of purity. Representative ^1H NMR spectra of $[\text{Ru}(\text{ptp})_2]^{2+}$ in comparison with that of its asymmetric ligand ptp are shown in Fig. 4. The proton chemical shifts are assigned with the aid of ^1H – ^1H COSY experiments and comparison with those of similar compounds.^{3,10,13,23}

As expected, on co-ordination of ligands to the ruthenium ion, the chemical shifts of H_a , H_b and H_c were shifted upfield. The pronounced shift for H_a is due to the magnetic anisotropy induced by the proximate ring current, but there is a lesser influence on H_b and H_c . On the other hand, H_d , H_e , H_f and H_g all show downfield shifts, and the overlapped signals for H_d and H_e are split into their individual resonances. This is the result of protons being in the deshielding region of the orthogonally ligand and has previously been studied for a series of annelated terpyridine ruthenium complexes.²⁴ In addition complexation has an influence on the chemical shifts of other protons in asymmetric ligands. As seen in Fig. 4, the chemical shifts of H_b , H_i , H_j and H_k on the biphenyl ring of ptp remain almost unchanged on co-ordination, however the protons on the biphenyl ring close to the metal ion all experience much larger shifts: H_i , H_m and H_n experience downfield shifts of 0.21–0.38 ppm while H_o shows a surprising downfield shift of 1.79 ppm in comparison with the corresponding protons of free ptp. This may be also attributed to the magnetic anisotropy induced by the proximate ring current. Similar observations can be made for other ruthenium complexes containing dppt or pta.

Electrochemistry

The electrochemical behaviors of the complexes have been studied in CH_3CN by cyclic voltammetry. Results are collected in Table 3. Each complex exhibits a well shaped oxidation (one) and reduction (two or three) waves in the sweep range from –1.9 to +1.7 V. This pattern is common to most d^6 metal polypyridyl complexes where the redox orbitals are localized on

Table 3 Redox potentials for the ruthenium(II) complexes^a

Complex	$\text{Ru}^{\text{III}}\text{--Ru}^{\text{II}}$	Ligand reduction		
1	1.35	–0.83	–1.03	
2	1.40	–0.75	–0.95	
3	1.43	–0.74	–0.95	
4	1.35	–0.85	–1.37	–1.55
5	1.38	–0.75	–1.41	–1.57
6	1.39	–0.75	–1.43	–1.58

^a All complexes were measured in 0.1 M $\text{NBu}_4\text{ClO}_4\text{--CH}_3\text{CN}$; error in potentials ± 0.02 V; $T = 23 \pm 1$ °C; scan rate = 100 mV.

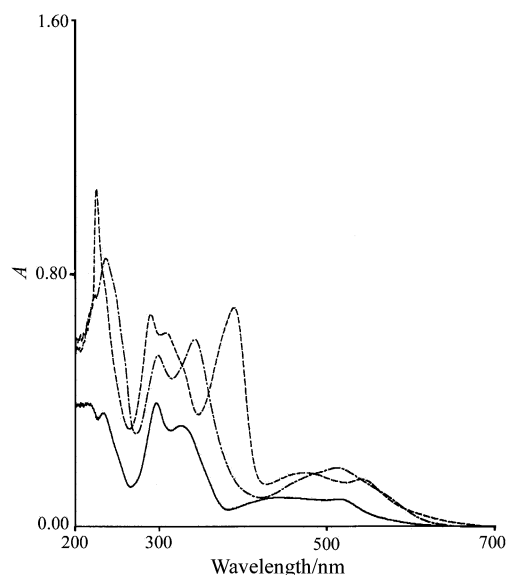


Fig. 5 The UV/VIS spectra of complexes **1** (—), **2** (---) and **3** (-.-) in acetonitrile.

the individual ligands.²⁵ The anodic and cathodic peak separations vary from 60 to 76 mV and are nearly scan rate independent, indicating that the processes are reversible one-electron transfers.

Oxidation of the complexes involves removal of an electron from the d_π orbital of Ru^{II} , while reduction involves removal of an electron to the ligand-centred orbitals. As seen in Table 3, the oxidations of the six complexes all shift to more positive potential in comparison with that of $[\text{Ru}(\text{tpy})_2]^{2+}$ (1.27 V).²⁶ This suggests that the better π^* acceptor character of the ligand (dppt, pta or ptp) stabilizes the ruthenium-based HOMO, rendering the oxidation of the metal more difficult. For all of the homoleptic complexes, the two reductions are attributed to two individual one-electron processes of the ligand (dppt, pta or ptp). This indicates that the extent of π delocalization of the asymmetric ligand increases in the order: dppt < pta \approx ptp. As to the heteroleptic complexes, the first reduction is obviously assigned to the asymmetric ligand, and the last two are characteristic of the ligand tpy.²⁶

Absorption spectra

Absorption spectra of the homoleptic complexes **1**, **2** and **3** were recorded in acetonitrile (Fig. 5). The spectra of the three complexes consist of four well resolved bands in the range 200 to 700 nm except for **2** for which a band at 390 nm is observed besides the four bands. The bands between 220 and 350 nm are attributed to intraligand (IL) $\pi\text{--}\pi^*$ transitions by comparison with the spectrum of $[\text{Ru}(\text{tpy})_2]^{2+}$.²⁶ Although the ligand pta exhibits an absorption band around 350 nm, it is replaced with a band at 390 nm in the spectrum of complex **2**. The increase in the absorption coefficient from pta to $[\text{Ru}(\text{pta})_2]^{2+}$, regarding the IL band of pta, suggests the band at 390 nm is a sum of the

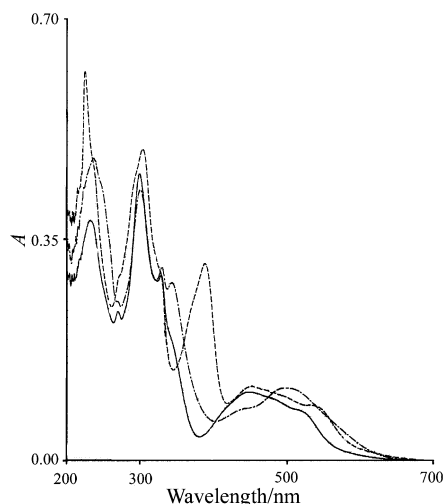


Fig. 6 The UV/VIS spectra of complexes **4** (—), **5** (---) and **6** (-.-) in acetonitrile.

pta π - π^* IL transition with other transitions of $[\text{Ru}(\text{pta})_2]^{2+}$. The lowest energy bands at 488, 506 and 512 nm for complexes **1**, **2** and **3** are assigned to the metal-ligand charge transfer (MLCT) transitions. These bands are bathochromically shifted by comparison with that of $[\text{Ru}(\text{tpy})_2]^{2+}$,²⁶ which reflects the strong π -acceptor character of the asymmetric ligands and their polyaromatic character.

Absorption spectra of the heteroleptic complexes **4**, **5** and **6** were also obtained in acetonitrile (Fig. 6). As observed in the electrochemistry, the energy of the π^* orbital in the asymmetric ligand is lowered with respect to that of terpyridine. Consequently, the Ru-to-L (L = dppt, pta or ptp) transitions are shifted to higher wavelength when compared to the Ru-to-tpy transition. For **4**, **5** and **6** two distinct MLCT bands might be expected. However, as a result of the broad nature of the bands and their relatively small wavelength separation, a broad MLCT band with shoulder peak is observed in the spectra of these complexes.

Acknowledgements

We thank the National Natural Science Foundation of China, the Natural Science Foundation of Guangdong Province, the State Key Laboratory of Coordination Chemistry in Nanjing University and the State Key Laboratory of Bio-organic and Natural Products Chemistry in the Shanghai Institute of Organic Chemistry for their financial support.

References

- E. A. Seddon and K. R. Seddon, *The Chemistry of Ruthenium*, Elsevier, Amsterdam, 1984; V. Balzani and F. Scandola, *Supramolecular Photochemistry*, Horwood, Chichester, 1991; A. Juris, V. Balzani, F. Barigelletti, S. Campagna, P. Belser and A. Von Zelewsky, *Coord. Chem. Rev.*, 1988, **84**, 85; K. Kalyanasundaram, *Coord. Chem. Rev.*, 1989, **28**, 2920; L. Fabbrizzi and A. Poggi (Editors), *Transition Metals in Supramolecular Chemistry*, Kluwer, Dordrecht, 1994; V. Balzani, A. Juris, M. Venturi, S. Campagna and S. Serroni, *Chem. Rev.*, 1996, **96**, 756; L. De Cola and P. Belser, *Coord. Chem. Rev.*, 1998, **177**, 301.
- J. P. Sauvage, J. P. Collin, J. C. Chambron, S. Guillerez and C. Coudret, *Chem. Rev.*, 1994, **94**, 993.
- E. C. Constable and M. D. Ward, *J. Chem. Soc., Dalton Trans.*, 1990, 1405; E. C. Constable, A. M. W. Cargill Thompson and D. A. Tocher, *New J. Chem.*, 1992, **16**, 855; E. C. Constable and A. M. W. Cargill Thompson, *J. Chem. Soc., Dalton Trans.*, 1992, 3467; N. Armaroli, V. Balzani, E. C. Constable, M. Maestri and A. M. W. Cargill Thompson, *Polyhedron*, 1992, **11**, 2707; E. C. Constable, C. E. Housecroft, M. Neuburger, A. G. Schneider and M. Zehnder, *J. Chem. Soc., Dalton Trans.*, 1997, 2427; G. Albano, V. Balzani, E. C. Constable, M. Maestri and D. R. Smith, *Inorg. Chim. Acta*, 1998, **277**, 225; E. C. Constable, C. E. Housecroft, E. R. Schofield and S. Encinas, *Chem. Commun.*, 1999, 869; E. C. Constable, J. E. Davies, D. Phillips and P. R. Raithby, *Polyhedron*, 1998, **17**, 3989.
- G. D. Storrer, S. B. Colbran and D. C. Craig, *J. Chem. Soc., Dalton Trans.*, 1997, 3011; G. D. Storrer, S. B. Colbran and D. C. Craig, *J. Chem. Soc., Dalton Trans.*, 1998, 1351.
- B. Whittle, S. R. Batten, J. C. Jeffery, L. H. Rees and M. D. Ward, *J. Chem. Soc., Dalton Trans.*, 1996, 424.
- C. R. Arana and H. D. Abruña, *Inorg. Chem.*, 1993, **32**, 194; L. M. Vogler and K. J. Brewer, *Inorg. Chem.*, 1996, **35**, 818; C. M. Hartshorn, N. Daire, V. Tondreau, B. Loeb, T. J. Meyer and P. S. White, *Inorg. Chem.*, 1999, **38**, 3200.
- A. Gourdon and J. P. Launay, *Inorg. Chem.*, 1998, **37**, 5336; P. Bonhôte, A. Lécas and E. Amouyal, *Chem. Commun.*, 1998, 885.
- B. Farlow, T. A. Nile, J. L. Walsh and A. T. McPhail, *Polyhedron*, 1993, **12**, 2891; E. C. Constable, A. J. Edwards, R. Martínez-Mañez, P. R. Raithby and A. M. W. Cargill Thompson, *J. Chem. Soc., Dalton Trans.*, 1994, 645; K. Hutchison, J. C. Morris, T. A. Nile, J. L. Walsh, D. A. Thompson, J. D. Petersen and J. R. Schoonover, *Inorg. Chem.*, 1999, **38**, 2516.
- M. Ziegler, V. Monney, H. Stoeckli-Evans, A. Von Zelewsky, I. Sasaki, G. Dupic, J. C. Daran and G. A. Balavoine, *J. Chem. Soc., Dalton Trans.*, 1999, 667.
- R. R. Ruminski, S. Underwood, K. Vallyly and S. J. Smith, *Inorg. Chem.*, 1998, **37**, 6528.
- R. Pickaert, M. Cesario, L. Douce and R. Ziessel, *Chem. Commun.*, 2000, 1125.
- N. W. Alcock, P. R. Barker, J. M. Haider, M. J. Hannon, C. L. Painting, Z. Pikramenou, E. A. Plummer, K. Rissanen and P. Saarenketo, *J. Chem. Soc., Dalton Trans.*, 2000, 1447.
- Y. Jahng, R. P. Thummel and S. G. Bott, *Inorg. Chem.*, 1997, **36**, 3133.
- B. P. Sullivan, J. M. Calvert and T. J. Meyer, *Inorg. Chem.*, 1980, **19**, 1404.
- E. J. Corey, A. L. Borror and T. Foglia, *J. Org. Chem.*, 1965, **30**, 288.
- A. C. T. North, D. C. Phillips and F. S. Mathews, *Acta Crystallogr., Sect. A*, 1968, **24**, 351.
- R. Blessing, *Acta Crystallogr., Sect. A*, 1995, **51**, 33.
- G. M. Sheldrick, SHELXS 97, Program for X-Ray Crystal Structure Determination, University of Göttingen, 1997; SHELXL 97, Program for X-Ray Crystal Structure Refinement, University of Göttingen, 1997.
- F. H. Case, *J. Org. Chem.*, 1966, **31**, 2398.
- C. K. Johnson, ORTEP II, Report ORNL-5138, Oak Ridge National Laboratory, Oak Ridge, TN, 1976.
- D. C. Craig, M. L. Scudder, W. A. Mchale and H. A. Goodwin, *Aust. J. Chem.*, 1998, **51**, 1131.
- B. H. Ye, X. M. Chen, T. X. Zeng and L. N. Ji, *Inorg. Chim. Acta*, 1995, **240**, 5.
- E. C. Constable and A. M. W. Cargill Thompson, *J. Chem. Soc., Dalton Trans.*, 1995, 1615.
- R. A. Thummel and Y. Jahng, *Inorg. Chem.*, 1986, **25**, 2527.
- S. Zails and V. Drchal, *Chem. Phys.*, 1987, **118**, 313.
- R. Berger and D. R. McMillin, *Inorg. Chem.*, 1988, **27**, 4245; P. R. Thummel and S. Chirayil, *Inorg. Chim. Acta*, 1988, **154**, 77.